Information circulation in a two-mode solid-state laser with optical feedback

Kenju Otsuka, Jing-Yuan Ko, Takayuki Ohtomo,* and Kazuyoshi Ohki
Department of Human and Information Science, Tokai University, 1117 Kitakaname, Hiratsuka, Kanagawa 259-1292, Japan
(Received 18 July 2001; published 30 October 2001)

A two-mode solid-state laser subjected to a delayed optical feedback is studied. Simultaneous random switchings between stable and chaotic antiphase spiking oscillations featuring the establishment of causal (drive response) relationships among modes have been demonstrated by a proposed *information circulation* analysis of an experimental time series. The observed phenomenon has been well reproduced by numerical simulations of two-mode laser equations with uncorrelated modal phase fluctuations.

DOI: 10.1103/PhysRevE.64.056239 PACS number(s): 42.60.Mi, 42.55.Rz, 89.70.+c

The nonlinear dynamics in coupled chaotic systems [1] has attracted much attention during the past decade. In particular, chaos synchronization phenomena have been demonstrated in many physical and biological systems. Most recently, Paluš *et al.* introduced an information-theoretic approach for studying synchronization behavior and identified causal (drive response) relationships between two coupled systems such as coupled Henon maps and brain tissues [2]. They showed that a synchronization phenomenon occurs as a result of an adjustment of information rates [2]. In optics, Heil *et al.* observed spontaneous symmetry breaking and the establishment of leader-lagger relationship in chaotic semiconductor lasers subjected to delayed face-to-face coherent optical coupling [3]. On the other hand, multimode lasers with delayed optical feedback have visited as promising systems for investigating deterministic dynamic interplay between coupled chaotic oscillators in connection with antiphase dynamics, in which the modal intensities can be antiphased [4,5].

In this paper, we extend the idea of ''direction of information flow'' by Paluš *et al.* and study a dynamic inter-mode interplay in a two-mode solid-state laser subjected to the common delayed optical feedback operating in the random chaotic bursting (RCB) state [6], in which the system exhibits switchings between the stable and chaotic operations. The RCB state is thought to be a prototypical example for investigating time-dependent drive-response relationships established in coupled chaotic oscillators. Here, we propose a dynamic information-theoretic quantity of *information circulation* to identify time-dependent information flows between two modes on the analogy of the gain circulation in multimode lasers that provides the underlying physical mechanism for antiphase dynamics, e.g., vanishing gain circulation rule [7]. We provide a theoretical evidence for *noise-mediate* antiphase random chaotic burst generations and identify the drive-response relationship between two modes established in the switching process arising from the cross saturation of population inversions. In addition, a comparison has been made between mode selective and common optical feedbacks and its connection with antiphase dynamics is discussed.

The experimental setup is shown in Fig. 1. We used a laser-diode (LD)-pumped 1-mm-thick $LiNdP_4O_{12}$ (LNP) laser. The input surface was coated to be antireflective at 808 nm and highly reflective (99.8%) for a 1000–1100 nm region. The output surface was coated to be reflective (99%) for the same wavelength region. When the pump power was increased from zero, single longitudinal-mode oscillation, which belongs to the ${}^4F_{3/2}(1) \rightarrow {}^4I_{11/2}(1)$ transition, appeared at 1048 nm. With the increase in the pump power, the second lasing mode appeared at 1055 nm that belongs to the ${}^4F_{3/2}(1) \rightarrow {}^4I_{11/2}(2)$ transition [8,9]. Experiments were carried out in this two-mode oscillation regime, in which single TEM_{00} mode oscillation was maintained. The output was linearly polarized at both wavelengths. The output light was divided into two beams and one beam (total output) was coupled to a 10 m single-mode fiber through a variable optical attenuator. A part of the total output was detected by an InGaAs photoreceiver with a 125 MHz bandwidth followed by a digital oscilloscope with a 500 MHz bandwidth. Another beam was splitted into two beams and modal outputs at 1048 nm and 1055 nm were passed through monochrometers. Each output was detected by InGaAs photoreceivers followed by the digital oscilloscope. The total and modal output wave forms were measured simultaneously and recorded by a personal computer. The experiment was carried out under the weak feedback condition of $C \equiv \kappa T_d \sqrt{1+\alpha^2} < 1$, where $\kappa = r_{ext}/\tau_L r_o(1-|r_o|^2)$ is the coupling strength and α is the linewidth enhancement factor. In this case, only single external cavity mode (ECM) exists in the vicinity of two solitary mode cavity frequencies. Here, τ_L is the roundtrip time within the LNP laser cavity, T_d is the delay time, r_{ext} is the amplitude reflectance for the feedback beam controlled by the attenuator, and r_o is the amplitude reflectivity of the LNP output mirror.

A typical example of observed wave forms is shown in Fig. 2(a) indicating the switching from the stable [i.e., relaxation oscillation (RO) driven by noise] to chaotic spiking oscillations (SO). Two points should be noted from this result; (1) chaotic bursting appears simultaneously in two modes, (2) two modes exhibit distinct antiphase dynamics. Corresponding power spectra are shown in Fig. 2(b). The lower relaxation oscillation frequency component at f_2 existing in the modal output is found to be suppressed for the total output. The latter result can be understood in terms of the inherent antiphase dynamics due to cross saturation of

*Present address: Department of Physics, Tokai University.

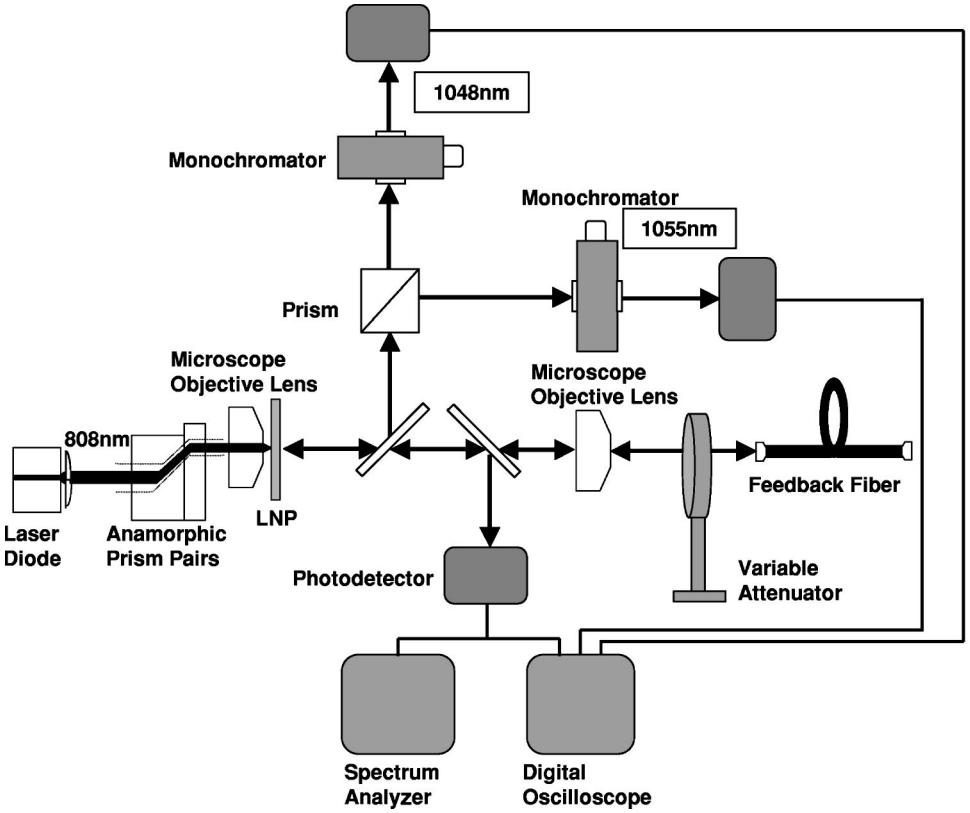

FIG. 1. Experimental setup of a LD-pumped two-mode LNP laser with feedback.

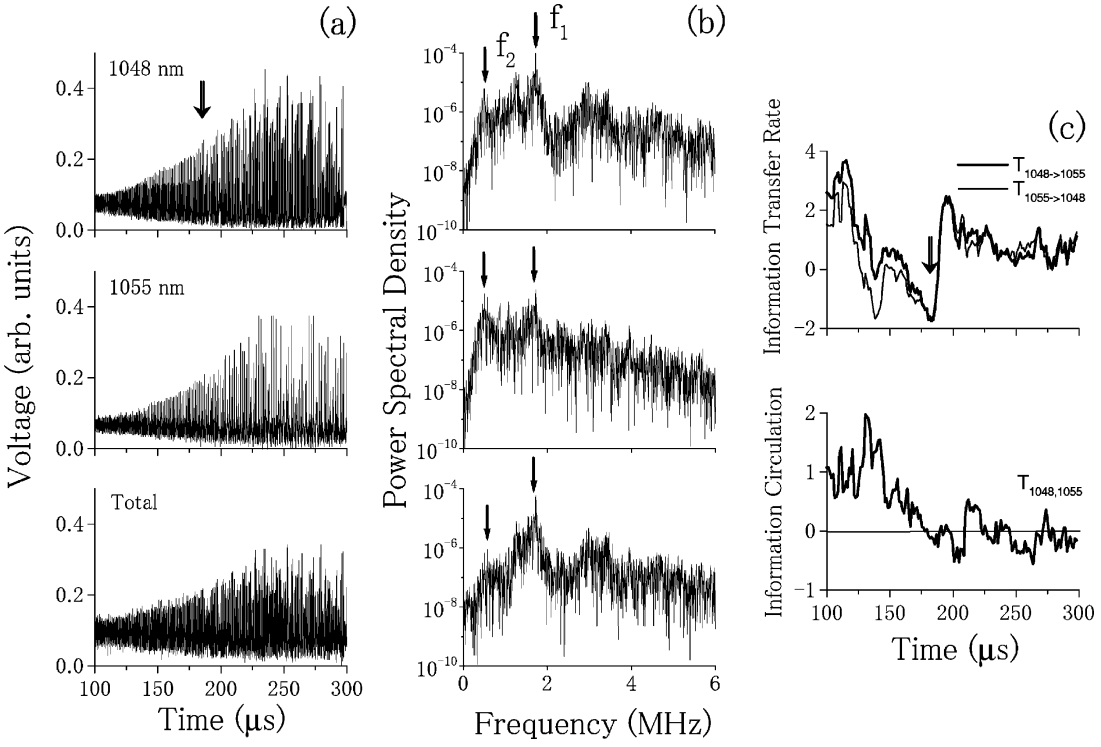

FIG. 2. Typical output characteristics of the switching behavior for a common optical feedback. (a) Intensities, (b) power spectra, and (c) information transfer rates and circulation. Information transfer rates and circulation were calculated by using a moving window of 1024 samples with a moving step of 128 samples [2].

population inversions [10]. The former result of *simultaneous chaotic bursting* suggests a degenerate Hopf bifurcation [5], however, it is not self-evident because two modes having different thresholds are not identical and two modes are expected to have different dynamic properties [11]. Then, an interesting question arises: *Which mode triggers the switching that leads to antiphase chaotic spikings?* To answer this question, we introduce the following information-theoretic dynamic quantity of *information circulation* to identify the information flows among modes on the analogy of gain and intensity circulations [7]:

$$T_{X,Y}=T_{X\to Y}-T_{Y\to X}, \tag{1}$$

where

$$T_{X\to Y}=\frac{1}{\tau^*}\sum_{\tau} S(Y,Y_\tau|X)-\frac{1}{\tau^*}\sum_{\tau} S(Y,Y_\tau), \tag{2}$$

is the information transfer rate from a time series $X=\{x(t)\}$ to $Y=\{y(t)\}$ [2,12], where $S(Y,Y_\tau)$ is the self-mutual information for Y [13,14]; i.e., a measure of the information (or predictability) that Y can provide about $Y_\tau=\{y(t+\tau)\}$. $S(Y,Y_\tau|X)$ is the conditional self-mutual information of the time series X given the time series Y. τ^* is the first local minimum of $S(Y,Y_\tau)$ [15]. When $T_{X,Y}>0(<0)$, the information flows from X (Y) to Y (X) similar to gain and intensity circulations [7].

Using this single dynamic quantity, we can identify the time-dependent change in a direction of information flow among modes by the use of experimental time series. The result of information circulation analysis of time series of Fig. 2(a) is shown in Fig. 2(c). In the stable (i.e., noise-driven RO) region before switching occurs, balanced bidirectional information flows are established among modes. In the switching region in Fig. 2(a), the 1048 nm mode becomes a drive that triggers the switching featuring a growing RO state, in which the information flows from the 1048 nm (drive) mode to the 1055 nm (response) mode. As the RO builds up enough, the system makes a transition to the chaotic SO state at the time indicated by ⇓. When the chaotic SO state is established, bidirectional information flow rates among two modes again tend to balance as shown in the upper figure of Fig. 2(c). At the same time, antiphase spiking oscillation is established featuring the strong suppression of the f_2 component for the total output as shown in Fig. 2(b). We have tested many switching events similar to Fig. 2(a) and confirmed the same scenario of time-dependent information flows, in which the 1048 nm mode having the lower threshold triggers the switching. *This implies that the strong* 1048 nm *mode always becomes a drive that triggers the switching in this case*.

Let us reproduce observed instability paying special attention on simultaneous chaotic bursting and casual (drive response) relationships between two modes that were observed experimentally. By introducing a modal feedback and a cross saturation due to the population inversion grating [8,9] into Lang-Kobayashi equations [16], we obtain

$$dS_k(t)/dt=K[g_kN_k(t)-\Gamma_k]S_k(t)+2\kappa_e\sqrt{S_k(t)S_k(t-t_d)}\cos\Theta_k(t)+F_{S,k}(t), \tag{3}$$

$$dN_k(t)/dt=W-N_k(t)-g_kN_k(t)[S_k(t)+\beta S_{k+1}(t)]+F_{N,k}(t), \tag{4}$$

$$d\phi_k(t)/dt=\Delta\Omega_k+\tfrac{1}{2}\alpha K[g_kN_k(t)-\Gamma_k]-\kappa_e\sqrt{S_k(t-t_d)/S_k(t)}\sin\Theta_k(t)+F_{\phi,k}(t), \tag{5}$$

$$\Theta_k(t)=\Omega_kt_d+\phi_k(t)-\phi_k(t-t_d),\quad k=1,2, \tag{6}$$

$$N_3=N_1,S_3=S_1,\phi_3=\phi_1,\Theta_3=\Theta_1,\Delta\Omega_3=\Delta\Omega_1. \tag{7}$$

Here, S_k is the normalized photon density, N_k is the population inversion density normalized by the threshold value, $W=P/P_{th}$ is the normalized pump power density, g_k is the gain ratio, Γ_k is the loss ratio, ϕ_k is the slowly varying part of the optical phase of the lasing field $E_k(t)\exp\{i[\omega_kt+\phi_k(t)]\}$, and Θ_k is the phase difference between the lasing field and the reinjected field. $\Omega_k=\Omega_{0,k}+\Delta\Omega_k$ $(k=1,2)$, where $\Omega_k=\omega_k\tau$ is the normalized optical angular frequency of ECMs and $\Omega_{0,k}=\omega_{0,k}\tau$ is the normalized optical angular cavity frequency of the kth solitary laser mode (τ: fluorescence lifetime). The coupling strength is normalized as $\kappa_e=\kappa\tau$. In the rate equations, the time has been normalized by the fluorescence lifetime τ, $K=\tau/\tau_p$ (τ_p: photon lifetime) is the time ratio, and t_d is the delay time. Here we assume cross-saturation parameter of $\beta=2/3$, $g_1=1$, $g_2=0.5$, $\beta=0.67$, $\Gamma_1=1$, and $\Gamma_2=0.733$ [8,9]. $F_{S,k}$, $F_{N,k}$, and $F_{\phi,k}$ are uncorrelated Gaussian white noises that satisfy $\langle F_{i,k}(t)\rangle=0$ and $\langle F_{i,k}(t)F_{j,k}(t')\rangle=2D_{ij}\delta(t-t')$. The angular bracket denotes ensemble average and D_{ij} is the diffusion coefficient associated with the corresponding noise source. Here, the subscript $i,j=S,N,\phi$.

The stationary solutions of Eqs. (3)–(5) are ECMs. The optical angular frequencies Ω_k of ECMs are the solution of

$$\Delta\Omega_kt_d+C\sin(\Omega_kt_d+\tan^{-1}\alpha)=0. \tag{8}$$

The steady-state characteristics can be characterized by C. In the case of $C<1$ as in the present experimental condition, there exists only one ECM in the vicinity of each solitary laser cavity frequency. In the absence of cross saturation (i.e., $\beta=0$), each ECM solution is not always dynamically stable and its stability changes depending on $\Delta\Omega_kt_d$ in Eq. (8) [16]. In short, the dynamical stability of ECM depends critically on the solitary laser cavity-frequency $\Omega_{0,k}$ in a large delay case. When the mutual coupling through cross saturation of population inversions is introduced, however, the dynamic stability of the coupled system is expected to change depending on $[\Delta\Omega_1,\Delta\Omega_2]$ for a given C. Therefore, in real experiments, it is expected that frequency fluctuations (i.e., phase noise) $\delta\omega_{0,k}$ are thought to result in random switching between stable and unstable states in time.

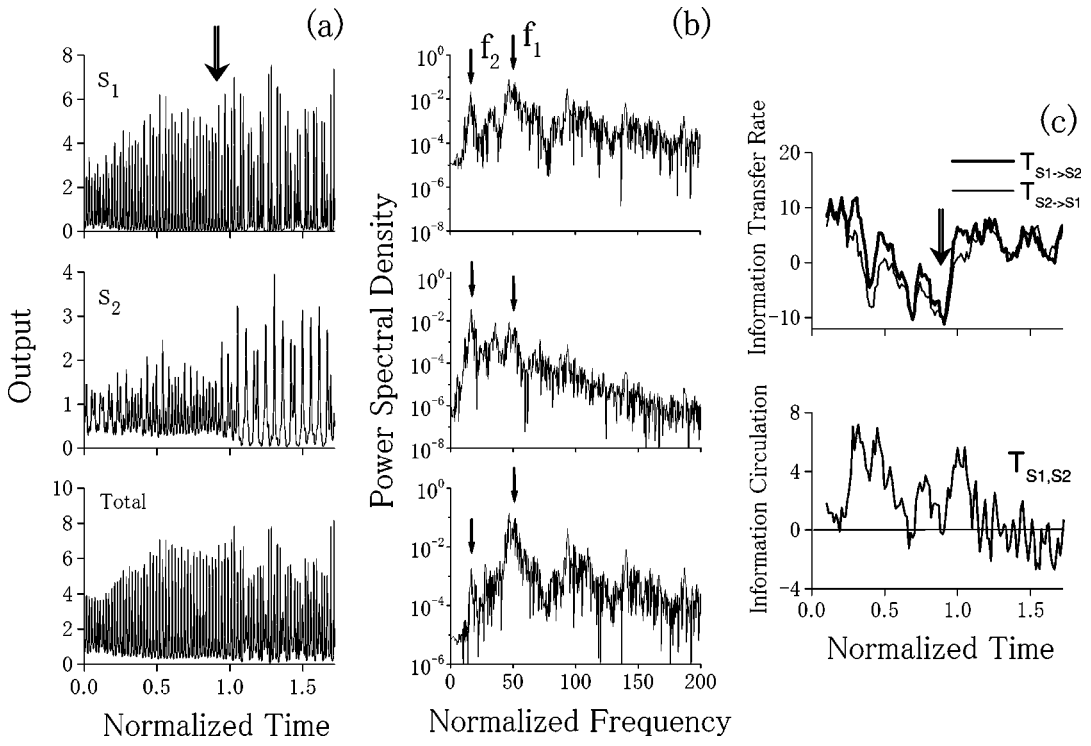

FIG. 3. Numerical result for nonidentical modes. (a) Intensities, (b) power spectra, and (c) information transfer rates and circulation. Adopted parameters: $K=10^5$, $\kappa_e=27$, $t_d=10^{-3}$, $W=2.5$, $\Delta\Omega_1=1.34$, $\Delta\Omega_2=0.81$, $\Omega_1=2.16\times10^{11}$, $\Omega_2=2.14\times10^{11}$, $\alpha=2$, and $D_{\phi,\phi}=30$. The condition for calculating information transfer rates and circulation is the same as in Fig. 2.

Let us first examine the effect of noise on laser dynamics numerically. We tested the effect of three different types of noise in dynamical equations and found that uncorrelated phase noise in Eq. (5) can well reproduce observed random switching between RO and chaotic SO states as expected. As for other noises in photon density (e.g., spontaneous emission noise) and population inversion density (e.g., pump noise), only degradation in the deterministically generated SO state occurred and no clear switching between two states was obtained. A typical numerical result indicating the simultaneous switching from a RO state driven by noise to a chaotic SO state is shown in Fig. 3(a). This simultaneous bursting parallels the experimental result. Corresponding power spectra reproducing the observed antiphase chaotic spiking oscillations are shown in Fig. 3(b), in which the f_2 component is strongly suppressed for the total output.

Calculated information transfer rates and the resultant information circulation are shown in Fig. 3(c). Obviously, the strong mode becomes a drive transiently that triggers the switching and a nearly symmetric information flow among the modes is established in the antiphase spiking region similar to the experiment. The quantitative agreement between the experiment and the numerical result shows that when the system enters the dynamic unstable region in the $[\Delta\Omega_1,\Delta\Omega_2]$ space by phase noise and the information transfer occurs from the strong mode to the weak mode transiently. We have numerically examined growth rates of periodic oscillation amplitudes for two modes starting from the vicinity of stationary solutions above a Hopf bifurcation point. It is found that the growth rate of an infinitestimal deviation from the steady-state value ΔS_k for the strong mode is larger than that for the weak mode, where $\Delta S_k(t)=\mathrm{Re}[\Sigma_s\sqrt{P(S_k,\omega_s)}\exp(\lambda_s t)]$ $(s=1,2)$ assuming $\mathrm{Re}(\lambda_1)>\mathrm{Re}(\lambda_2)$ for real parts of complex conjugate eigenvalues [11] and the universal power spectra relation of $P(S_1,\omega_1)>P(S_2,\omega_1)$ and $(S_1,\omega_2)<P(S_2,\omega_2)$, where $P(S_s,\omega_s)$ is the power spectral density of the sth mode at frequency ω_s [17]. This implies that antiphase chaotic spiking oscillations that buildup from the noise-driven RO state are triggered by the strong mode owing to its larger growth rate and a drive-response relationship is formed in the growing RO region, featuring the information transfer from the strong mode to the weak mode.

Then, let us examine the case when identical modes involve in chaotic burstings numerically. Typical examples are shown in Fig. 4, assuming $g_1=g_2=1$ and $\Gamma_1=\Gamma_2=1$. The chaotic bursting occurs simultaneously for both modes similar to the nonidentical mode case as shown in Fig. 4(a), however, the drive-response relationship is not formed and balanced bidirectional information flows are established in the whole time region as shown in Fig. 4(c), featuring antiphase spiking oscillations shown in Fig. 4(b). This result implies the existence of a degenerate Hopf bifurcation [5] in the case of identical modes.

Finally, let us show the experimental result for a mode-selective optical feedback. The experiment was carried out by injecting one of the modal outputs into the optical fiber through the monochrometer, while the other mode is left in the free-running condition. Random chaotic burstings were observed when the strong 1048 nm mode was subjected to optical feedback and the coupling strength was increased by

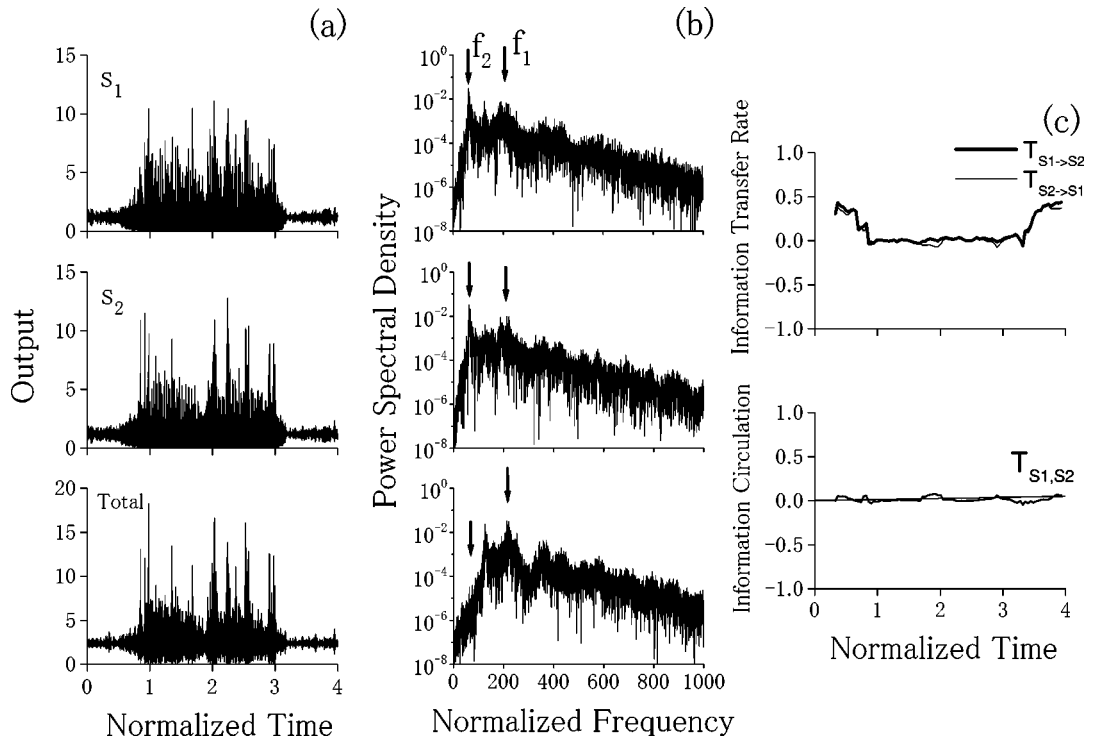

FIG. 4. Numerical result for identical modes. (a) Intensities, (b) power spectra, and (c) information transfer rates and circulation. $K=10^6$, $\kappa_e=150$, $t_d=1.5\times10^{-3}$, $W=3.0$, $\Delta\Omega_1=10$, $\Delta\Omega_2=15$, $\Omega_1=1.35\times10^{11}$, $\Omega_2=1.40\times10^{11}$, $\alpha=2$, and $D_{\phi,\phi}=14$. The condition for calculating information transfer rates and circulation is the same as in Fig. 2.

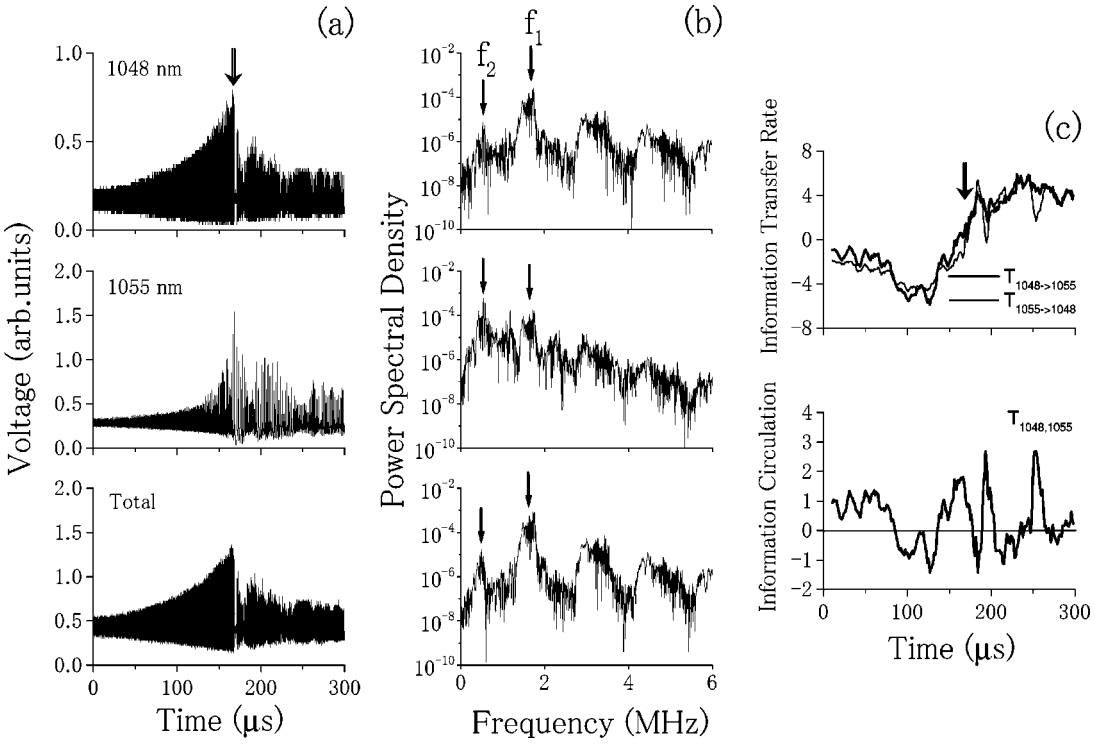

FIG. 5. Typical output characteristics of the switching behavior for a mode-selective optical feedback. The optical feedback was applied only to the 1048 nm mode. (a) Intensities, (b) power spectra, and (c) information transfer rates and circulation. The condition for calculating information transfer rates and circulation is the same as in Fig. 2.

10 dB as compared to the common feedback, while the weak 1055 nm mode feedback was not effective for bursting oscillations. The observed simultaneous chaotic bursting wave forms are shown in Fig. 5(a). It is interesting to note that the switching process is qualitatively different from that for the common feedback shown in Fig. 2. In particular, the clear transition from the RO state to the chaotic SO state at the time indicated by ⇓ in Fig. 2 does not occur and the chaotic SO state is replaced by smaller-amplitude chaotic relaxation oscillations as shown in Fig. 5(a). Furthermore, the antiphase dynamics is degradated as shown in power spectra of Fig. 5(b), in which the suppression of f_2 component for the total output is not sufficient. The drive-response relationship is established in the initial stage of switching behavior, however, a significant temporal change in the direction of information flow between two modes become apparent in the chaotic relaxation oscillation region as shown in Fig. 5(c). This may result from the violation of antiphase dynamics owing to the strong asymmetry of the system.

It should be mentioned that the present instability is observed by a delayed optical feedback from an external reflector instead of the single-mode fiber.

In conclusion, simultaneous random chaotic burst generations featuring antiphase dynamics and the establishment of drive-response relationships among modes have been demonstrated in a LD-pumped microchip two-mode LNP laser subjected to a delayed feedback by a proposed information circulation analysis of an experimental time series. The observed phenomenon has been well reproduced by numerical simulations of two-mode delay-differential laser equations including the cross saturation of population inversion densities and uncorrelated modal phase noise. The proposed method of information circulation analysis is shown to be the most effective for identifying the dynamic interplay among coupled chaotic oscillators in terms of direction of information flow. This methodology would be useful for characterizing complex behaviors in various physical and biological nonlinear systems possessing large coupled degrees of freedom.

[1] L.M. Pecora, T.L. Carrol, G.A. Johnson, and D.J. Mar, Chaos **7**, 520 (1997).
[2] M. Paluš, V. Komarek, Z. Hrncir, and K. Sterbova, Phys. Rev. E **63**, 046211 (2001).
[3] T. Heil, I. Fischer, W. Elsasser, J. Mulet, and C.R. Mirasso, Phys. Rev. Lett. **86**, 795 (2001).
[4] G. Vaschenko, M. Giudici, J.J. Rocca, C.S. Menoni, J. Tredicce, and S. Balle, Phys. Rev. Lett. **81**, 5536 (1998).
[5] E.A. Viktorov and P. Mandel, Phys. Rev. Lett. **85**, 3157 (2000).
[6] K. Otsuka, J.-Y. Ko, J.-L. Chern, K. Ohki, and H. Utsu, Phys. Rev. A **60**, R3389 (1999).
[7] K. Otsuka and Y. Aizawa, Phys. Rev. Lett. **72**, 2701 (1994).
[8] K. Otsuka, R. Kawai, Y. Asakawa, P. Mandel, and E.A. Viktorov, Opt. Lett. **23**, 201 (1998).
[9] R. Kawai, Y. Asakawa, and K. Otsuka, IEEE J. Quantum Electron. **QE-35**, 1542 (1999).
[10] K. Otsuka, *Nonlinear Dynamics in Optical Complex Systems* (Kluwer Academic Publishers, Dordrecht, 1999).
[11] B.A. Nguyen and P. Mandel, Quantum Semiclassic. Opt. **1**, 320 (1999).
[12] T. Schreiber, Phys. Rev. Lett. **85**, 461 (2000).
[13] K. Ikeda and K. Matsumoto, Phys. Rev. Lett. **62**, 2265 (1989).
[14] J.-L. Chern, Phys. Rev. E **50**, 4315 (1994).
[15] A.M. Fraser and H.L. Swinney, Phys. Rev. A **33**, 1134 (1986).
[16] R. Lang and K. Kobayashi, IEEE J. Quantum Electron. **QE-16**, 347 (1980).
[17] P. Mandel, K. Otsuka, J.-Y. Wang, and D. Pieroux, Phys. Rev. Lett. **76**, 2694 (1996).